

COMBINED POPULATION BALANCE AND CFD MODELLING OF PARTICLE AGGREGATION BY POLYMERIC FLOCCULANT

Alex R. HEATH and Peter T.L. KOH

A.J. Parker Cooperative Research Centre for Hydrometallurgy
 (CSIRO Minerals), Clayton South, Victoria, Australia

ABSTRACT

A population balance model has been incorporated into CFD to model particle aggregation in solid/liquid separation systems. The model is written specifically to describe flocculation by high molecular weight polymer flocculants, and includes terms to describe the rates of flocculant/suspension mixing and adsorption, particle collision to form aggregates, and partially irreversible aggregate breakage. These rates are all functions of the local turbulent shear rate, flocculant and particle concentrations, which are in turn predicted by the CFD code. Hence the combined population balance/CFD model gives the local aggregate size distribution, which varies considerably across the vessel depending on the local conditions.

The fluid model is turbulent two-phase Eulerian/Eulerian, using the $k-\varepsilon$ turbulence model which also gives an estimate of local turbulent shear rate from $(\varepsilon\rho/\mu)^{0.5}$. The population balance consists of 35 particle size channels solved as scalar equations in CFX4. Although this dramatically increases the number of equations at each node point, the population balance equations converge rapidly compared to the flow equations. Hence faster overall convergence is possible by only solving the additional population balance equations in the last couple of hundred iterations.

NOMENCLATURE

a	Particle radius (m)
G	Spatially averaged shear rate (s^{-1})
N	Number of particles (m^{-3})
S	Breakage rate (breakage kernel) (s^{-1})
t	Time (s)
v	Volume of particle (m^3)
α	Particle capture/collision efficiency [0,1] (dimensionless)
β	Particle collision rate (aggregation kernel) ($m^3 s^{-1}$)
ψ	Breakage distribution function (dimensionless)
ε	Energy dissipation rate ($m^2 s^{-3}$)
ν	Kinematic viscosity ($m^2 s^{-1}$)
ρ	Density ($kg m^{-3}$)
Γ	Diffusivity ($kg m^{-1} s^{-1}$)
U	Fluid velocity ($m s^{-1}$)
ϕ	Volume fraction ($m^3 m^{-3}$ – dimensionless)

Subscripts

i, j or k	Particle size channels
s	Solid phase

INTRODUCTION

Population balances are widely used to model dynamic particle or droplet size distributions, for example: aggregation, flocculation, crystallisation, bubble or droplets in solvent extraction or flotation columns, size distributions in comminution or grinding circuits. Essentially, a population balance models a size distribution by discretising the size range, resulting in a system of differential equations that describes the rate of accumulation or loss of particle number or mass in each of the size categories or channels. A population balance may contain aggregation or breakage rate terms, or both.

Analytical solutions have been proposed for either simple aggregation or breakage kinetics separately, but more complex behaviour or simultaneous aggregation and breakage generally requires a numerical solution. Not surprisingly, most population balance research is fairly recent, with computational speed now sufficient to make a combined population balance-CFD (PB-CFD) approach viable. I.e., the full population balance is solved at each node point in the CFD mesh as a function of the local conditions, and with the population balance scalars also simultaneously convected and diffused through the flow.

Smoluchowski (1916, 1917) first proposed the population balance, including only aggregation terms:

$$\frac{dN_k}{dt} = \frac{1}{2} \sum_{i=1, i+j=k}^{k-1} \beta_{ij} N_i N_j - \sum_{i=1}^{\infty} \beta_{ik} N_i N_k \quad (1)$$

β_{ij} is the aggregation rate between the i^{th} and j^{th} sized particles, a size dependent rate term referred to as a kernel in the population balance. Aggregation may be caused by a number of collision mechanisms simultaneously, Brownian motion (mostly smaller particles), differential settling (particles of different size or density) or turbulent collision. In industrial scale turbulent flows turbulent collision is usually dominant to the extent that the other mechanisms are ignored. The collision rate of neutrally buoyant spherical particles smaller than the Kolmogoroff microscale is given by Saffman and Turner (1955):

$$\beta_{ij} = 1.29G(a_i + a_j)^3 \quad (2)$$

Where G is the turbulent shear rate and the bracketed term the particle collision radius. A wide variety of other turbulent collision kernels have also been proposed, but Equation 2 remains the most popular. The kernel has been used successfully to model a range of physical systems, usually in conjunction with a capture efficiency term to account for unsuccessful collisions due to electrostatic or hydrodynamic repulsion.

Aggregates may also break up again and additional terms are frequently added (Lick and Lick 1988):

$$\begin{aligned} \frac{dN_k}{dt} = & \frac{1}{2} \sum_{i=1, i+j=k}^{k-1} \alpha_{ij} \beta_{ij} N_i N_j - \sum_{i=1}^{\infty} \alpha_{ik} \beta_{ik} N_i N_k \\ & - S_k N_k + \sum_{i=k+1}^{\infty} \psi_{ik} S_i N_i \end{aligned} \quad (3)$$

In order to reduce the number of differential equations, the particle size interval is discretised, in this case according to (Batterham *et al.* 1981):

$$\frac{v^{i+1}}{v^i} = 2 \quad (4)$$

resulting in (Hounslow *et al.* 1988, Spicer and Pratsinis 1996):

$$\begin{aligned} \frac{dN_i}{dt} = & \sum_{j=1}^{i-2} 2^{j-i+1} \beta_{i-1,j} N_j + \frac{1}{2} \beta_{i-1,i-1} N_{i-1}^2 - N_i \sum_{j=1}^{i-1} 2^{j-i} \beta_{i,j} N_j \\ & - N_i \sum_{j=1}^{\infty} \beta_{i,j} N_j - S_i N_i + \sum_{j=i}^{\infty} \Gamma_{i,j} S_j N_j \end{aligned} \quad (5)$$

EXPERIMENTAL

The aggregation/breakage kinetics of calcite particles (mean vol. wtd. diameter 16 μm) flocculated with a high molecular weight 30 % anionic flocculant were studied in turbulent pipe (22 mm ID) flow. A variety of different lengths of pipe were used between the flocculant addition point and the in-stream aggregate sizing probe at the other end of the pipe, i.e. giving a range of mean flocculation residence times assuming plug flow.

Aggregate sizing was with a Lasentec M500 Focused Beam Reflectance Measurement (FBRM) probe placed directly into the flow. The instrument gives a particle chord, rather than conventional diameter distribution, and details of calibration work against conventional sizing techniques/instruments like sieves, Malvern Mastersizer and Coulter Counter can be found in Heath *et al.* (2002).

A range of different pipe flow rates were used to produce different turbulent shear rates, with a turbulent pipe chosen over other possible reactor geometries (Couette flow, stirred baffled tank etc) due to the relatively homogeneous turbulent shear, easily calculated mean residence time, and well understood fluid behaviour.

POPULATION BALANCE DEVELOPMENT

Before its inclusion as a sub-model in the CFD code, the population balance model was developed from pipe reactor experimental data. This included aggregation and breakage kernel formulation and model parameter estimation. Due to the number of simulations required for the model development, full CFD simulations would have been too slow, and a commercial differential equation solver (gPROMS) was used instead. In this case the population balance was solved as a time-marching initial value problem, corresponding to the (plug) flow of aggregating suspension down the pipe. The reaction was taken to be single-dimensional, i.e. homogeneous across the pipe.

A typical modelling approach was taken, using the turbulent collision kernel by Saffman and Turner (1955) (Equation 2), in conjunction with a capture efficiency term and a breakage kernel. I.e., the modelled capture

efficiency and breakage terms are adjusted to give a good fit to the experimental data.

In this case the breakage kernel by Spicer and Pratsinis (1996) was used:

$$S_i = P G^Y a_i \quad (6)$$

where:

$$G = \sqrt{\frac{\epsilon}{\nu}} \quad (7)$$

and P and Y are fitted parameters. Similar breakage kernels have been used elsewhere (Parker 1972, Serra and Casamitjana, 1998, Chung *et al.* 1998, Young *et al.* 2000) to describe aggregation systems, with the value of Y typically being found to be ~1.5-2. Parameter Y essentially sets the model's behaviour in relation to changes in the shear rate (G), i.e. the aggregation rate is taken to be proportional to $G^{1.0}$ whereas the breakage rate is raised to a higher power, consistent with the typical experimental result that a higher shear rate gives a faster initial aggregate growth, but ultimately produces smaller aggregates due to the increased (and dominant) breakage rate.

Aggregation by high molecular weight polymer flocculants (as widely used in mineral processing thickeners or clarifiers) differs from aggregation by ionic coagulants (typical of water treatment clarifiers, or natural systems like estuaries). Although polymer flocculants typically produce larger and faster settling aggregates, the aggregates formed are subject to irreversible breakage due to polymer chain scission or rearrangement. This behaviour is shown by the gentle decrease in the aggregate size on extended reaction times in Figure 1. Aggregates formed by coagulation on the other hand are able to re-form and typically achieve a constant steady-state aggregate size.

Breakage irreversibility was introduced into the model by making the particle capture efficiency term decrease through time, reflecting the loss of flocculant activity due to polymer scission or rearrangement:

$$\alpha = C e^{-t/D} \quad (8)$$

where C is the initial capture efficiency and D is a parameter for the rate of decrease in the capture efficiency with time (t). In this case, C and D are fitted parameters. Equation 8 is likely to be simplistic, and should also probably be written as a function of other variables like the shear rate, solid fraction, particle size, flocculant molecular weight, etc. However, the current function produced a good fit with the available experimental data (Figure 1). Model parameter estimation (fitting) was achieved with a conventional sum-of-squares minimisation, in this case between the modelled and experimental mean aggregate diameters at the various positions along the pipe reactor:

$$\min_{C,D,P,Y} \phi = \sum_{G=l,m,h} \sum_{t=0}^{\infty} \left(\bar{a}_{\text{expt}} - \bar{a}_{\text{model}} \right)^2 \quad (9)$$

giving values of C = 0.635, D = 150, P = 1.23 and Y = 1.88.

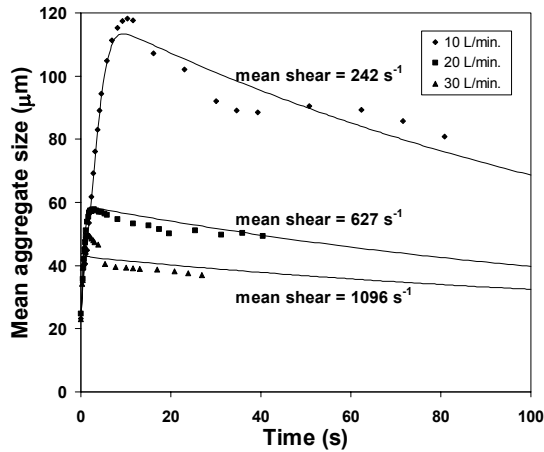


Figure 1: Comparison of modelled and experimental mean aggregate size as a function of aggregation time along pipe reactor using the 1-D model in gPROMS.

CFD DEVELOPMENT

A two-continuum Eulerian-Eulerian technique is used in the two-phase flow calculations. One set of continuity and momentum equations are solved for each of the solid and liquid phases, and the two sets of equations are coupled by means of a common pressure field and inter-phase momentum exchange terms. Turbulence is modelled using the $k-\epsilon$ turbulence model which also gives an estimate of local turbulent shear rate from $(\epsilon\rho/\mu)^{0.5}$. The population balance consists of 35 particle size channels solved as scalar equations in CFX-4. The mass error in the population balance is less than 0.04 wt% per iteration. The size fractions are re-normalised after each iteration step to conserve mass. The flocculant mixing and adsorption model in the CFD model can predict polymer coverage on the particle surface. This is linked to the probability of capture needed in the population balance model. Because of the relative rates of mixing and adsorption in comparison with the flocculation processes, the aggregation kinetics in the model are switched on only when the polymer coverage exceeds a certain value of the particle surface. This approximation allows for an aggregation rate of zero when the polymer adsorption on the particles is less than the required coverage. The capture efficiency in the flocculation kinetics in Equation 8 was proposed for the pipe reactor where the time elapsed is approximately known assuming plug flow. In the steady-state CFD model, the equation for the capture efficiency is replaced by a differential source term as follows:

$$\frac{d\alpha}{dt} = -\frac{\alpha}{D} \quad (10)$$

and an initial condition of $\alpha = C$ at $t = 0$, or the flocculant addition point. This modification is applied to account for the mixing of aggregates of different ages because of irreversible breakage and re-aggregation. Overall the CFX-4 code solves:

$$\nabla \cdot [\phi(\rho_s \mathbf{U}_s \alpha - \Gamma \nabla \alpha)] = \phi \rho_s \frac{\alpha}{D} \quad (11)$$

Transport equations similar to Equation 11 are solved for the flocculant and population balance scalars, with the

appropriate source terms given by either the flocculant adsorption model or the population balance (Equation 5).

POPULATION BALANCE AND CFD SIMULATIONS

Pipe reactor model

The population balance model has been successfully implemented in CFD as demonstrated by Figure 2. Because of wall boundary layers, a profile of shear rates based on Equation 7 was obtained for the pipe reactor. The volume-averaged shear rate as calculated from the $k-\epsilon$ model is somewhat lower than the shear rate obtained from pressure drop correlations. The four parameters (C , D , P and Y) in the flocculation kinetics model have been obtained with shear rates from the pressure drop correlation. An adjustment is necessary when the local shear rate calculated from the $k-\epsilon$ model is used in the flocculation kinetics model in the CFD model.

However, Figure 2 shows that the population balance model has been successfully transferred from gPROMS (Figure 1) where it was solved as a single-dimensional time marching simulation to CFX-4, where it is solved as a steady-state two-phase three-dimensional model.

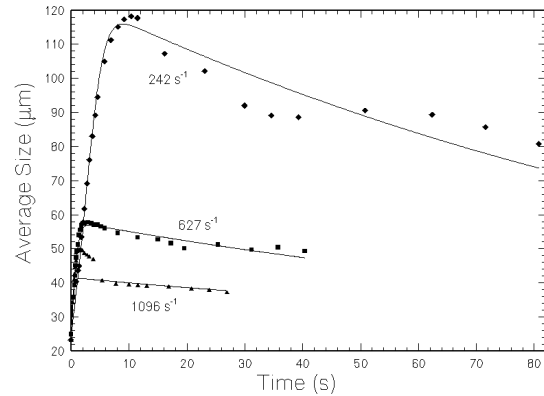


Figure 2: Comparison between CFX-4 predicted and measured average aggregate sizes in the pipe reactor.

Thickener feedwell model

The arrangement of a simulated full-scale industrial thickener feedwell is shown in Figure 3. The arbitrary thickener feedwell dimensions and operating conditions used in the simulation were as follows:

- Open feedwell with a single inlet entering tangentially;
- Thickener: 30 m diameter and 6 m height;
- Feedwell: 6 m diameter and 3 m height;
- Feedpipe: 600 mm diameter located at 1 m below surface;
- Volumetric flow rate $2000 \text{ m}^3 \text{ h}^{-1}$ and average inlet flow velocity 2 m s^{-1} ;
- Viscosity of $10^{-6} \text{ m}^2 \text{ s}^{-1}$ and solids density of 2900 kg m^{-3} ;
- Feed solids concentration of 6 wt%;
- Diameter of primary feed particles of 24 μm ;
- Flocculant rate of $50 \text{ m}^3 \text{ h}^{-1}$ and flocculant concentration of 0.3 wt%;
- Flocculant sparge at 1m below surface.

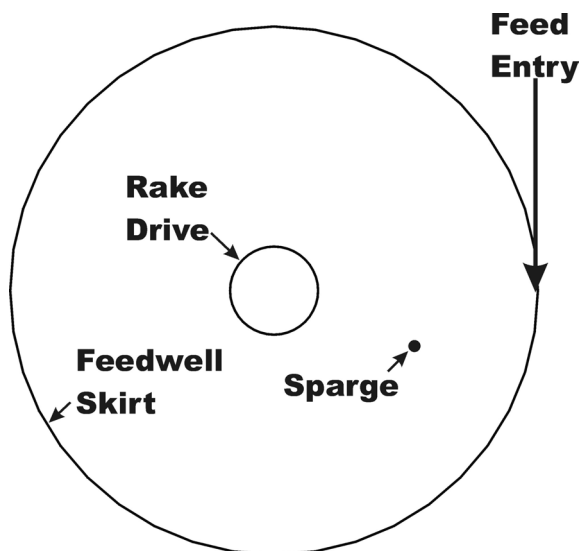


Figure 3: Schematic of the feedwell with a tangential feed entry and sparge for flocculant addition.

In the simulation presented in this section, only the feedwell with a grid of 40x14x15 is simulated as an example of the population balance-CFD model. Grid refinement was not attempted in this example since the aim at this stage of the work was to develop and refine the population balance model with the CFD framework. At the bottom of the open feedwell, a mass-flow boundary condition was applied allowing the flow to exit the feedwell. There is no dilution stream across this boundary from the bulk of the thickener.

The population balance-CFD results are presented in Figures 4 to 6 in terms of the distribution of solids, adsorbed flocculant, velocities, mass fraction of the remaining primary particles, and mean aggregate diameter. These results have been obtained during the solving of all transport equations and not during post-processing. The decay in the capture efficiency with distance at the feed entry level is also shown in Figure 5.

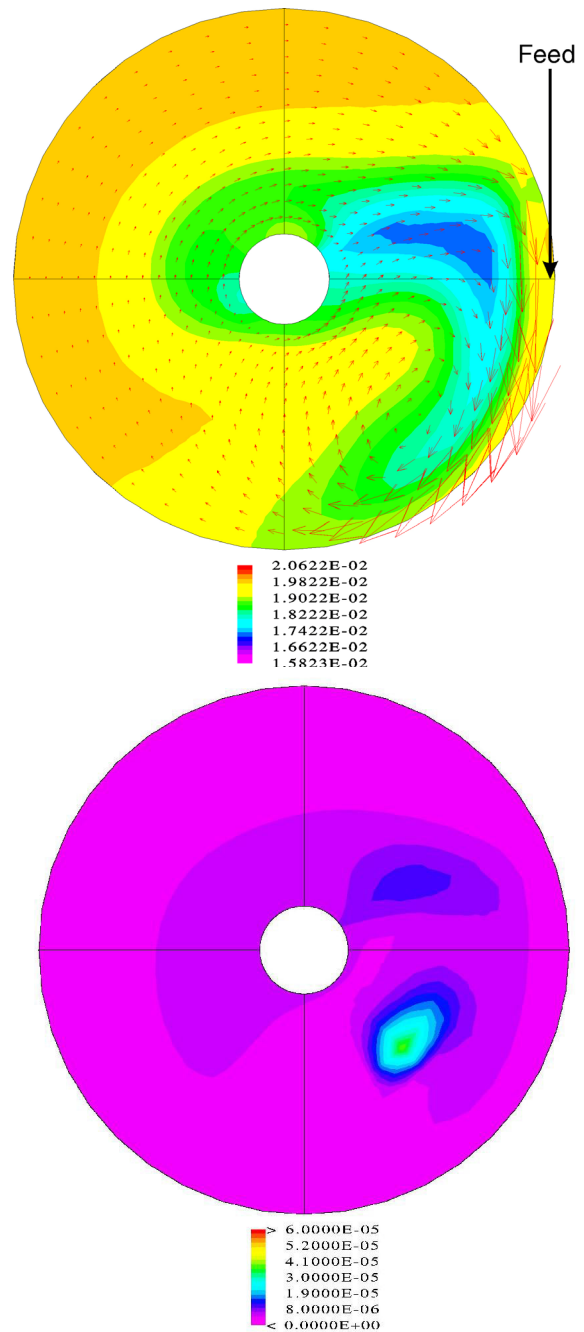


Figure 4: Solids distribution (top) (as solid volume fraction), velocity vectors, and adsorbed flocculant concentration (bottom) (as mass fraction) at the feed entry level in the simulated thickener feedwell.

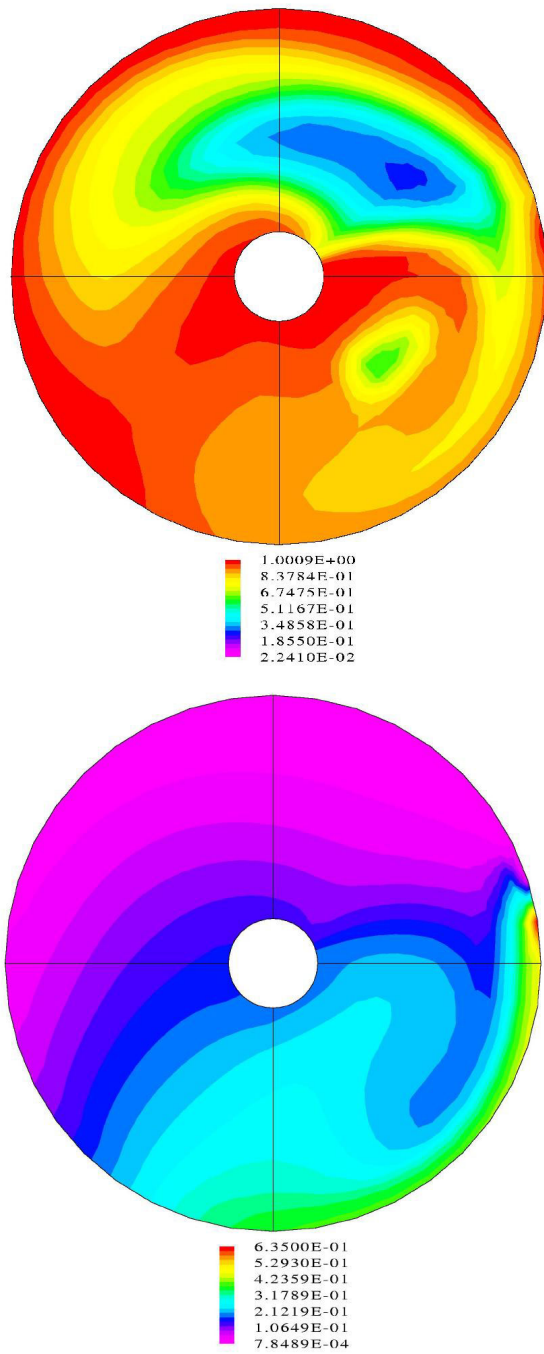


Figure 5: Mass fraction of primary particles (top) and capture efficiency (bottom) at the feed entry level in the simulated thickener feedwell.

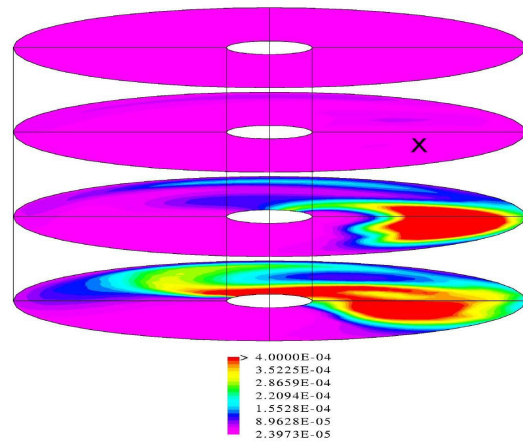


Figure 6: Average size (units: m) of aggregates from predicted size distributions at four levels in the simulated thickener feedwell: at 0, 1, 2 and 3 m from the surface. Sparge exit marked by X.

The plots show that aggregation occurs near the sparge exit, as indicated by a high flocculant adsorption shown in Figure 4 and the large aggregate sizes shown in the feedwell (Figure 6).

The cumulative size distributions in Figure 7 indicate that the aggregates increase in size with increasing distance from the sparge exit. Also, the larger aggregates are found over a wider region with increasing distance from the sparge.

The population balance CFD model can be used to distinguish how different sparge locations may affect the size of aggregates produced in the feedwell, i.e. it has passed the proof-of-concept stage. The model can of course be improved by including other features, e.g. the dilution stream from the bulk of the thickener and this is currently being done within the AMIRA P266D “Improving Thickener Technology” project.

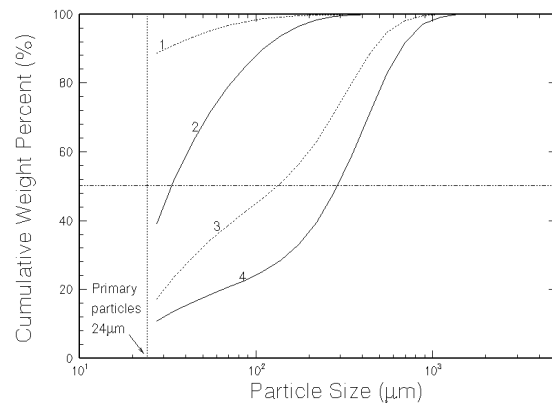


Figure 7: Particle size distributions at four positions within the thickener feedwell: (1) at feed entry, (2) at sparge exit, (3) at 1 m below sparge, and (4) at 2 m below sparge. Average sizes obtained for these positions are 29.1, 52.4, 192 and 317 μm respectively.

CONCLUSIONS

A population balance for polymer flocculation has been formulated for simulation of feedwell performance in thickeners and clarifiers. The population balance includes terms describing aggregation and partially irreversible breakage and was developed from experimental data from turbulent pipe flow.

The population balance was coded into CFX-4 as an additional 35 transported scalar equations describing the number density of particles in a given size range. In addition, two extra transported scalars were included - the flocculant concentration and a capture efficiency term accounting for the loss of flocculant activity through time. The model gives the opportunity to optimise thickener design by giving sufficient shear and residence time to ensure adequate flocculant/feed mixing and subsequent particle aggregation, but avoid regions of excessive shear that cause irreversible aggregate breakage.

ACKNOWLEDGEMENTS

This research has supported by the Australian Government's Cooperative Research Centre (CRC) program, through the AJ Parker CRC for Hydrometallurgy. Support was also provided by the AMIRA P266C "Improving Thickener Technology" project.

REFERENCES

- BATTERHAM, R.J., HALL, J.S. and BARTON, T. (1981), 'Pelletizing kinetics and simulation of full scale balling circuits', 3rd International Symposium on Agglomeration, pp. A136-A151.
- CHUNG, C.B., PARK, S.H., HAN, I.S., SEO, I.S. and YANG, B.T. (1998), 'Modelling of ABS latex coagulation processes', *AIChE Journal*, Vol. 44, No. 6, pp. 1256-1265.
- HEATH, A.R., FAWELL, P.D., BAHRI, P.A. and SWIFT, J.D. (2002), 'Estimating average particle size by focussed beam reflectance measurement (FBRM)', *Particle and Particle Systems Characterisation.*, Vol. 19, pp. 84-95.
- HOUNSLOW, M.J., RYALL, R.L. and MARSHALL, V.R. (1988), 'A discretized population balance for nucleation, growth and aggregation', *AIChE Journal*, Vol. 34, No. 11, pp. 1821-1832.
- LICK, W. and LICK, J. (1988), 'Aggregation and disaggregation of fine-grained lake sediments', *J. Great Lakes Res.*, Vol. 14, No. 4, pp. 514-523.
- PARKER, D.S., KAUFMAN, W.J. and JENKINS, D. (1972), 'Floc breakup in turbulent flocculation processes', *Journal of the Sanitary Engineering Division, Proceedings of the American Society of Civil Engineers*, Vol. 8702, pp. 79-99.
- SAFFMAN, P. and TURNER, J. (1955), 'On the collision of drops in turbulent clouds', *J. Fluid Mechanics*, Vol. 1, pp. 16-30.
- SERRA, T. and CASIMITJANA, X. (1998), 'Modelling the aggregation and break-up of fractal aggregates in a shear flow', *Applied Scientific Research*, Vol. 59, No. 2-3, pp. 255-268.
- SMOLUCHOWSKI, M. (1916), 'Drei Vorträge über die Diffusion, Brownsche Bewegung und Koagulation von Kolloidteilchen', *Physik Zeitschrift*, Vol. 17, pp. 557.
- SMOLUCHOWSKI, M. (1917), 'Versuch einer mathematischen Theorie der Koagulationskinetik kolloider Lösungen', *Z. Phys. Chem.*, Vol. 92, pp. 129-168.
- SPICER, P.T. and PRATSINIS, S.E. (1996), 'Coagulation and fragmentation: Universal steady-state particle-size distribution', *AIChE Journal*, Vol. 42, No. 6, pp. 1612-1620.
- YOUNG, S., STANLEY, S.J. and SMITH, D.W. (2000), 'Effect of mixing on the kinetics of polymer aided flocculation', *Journal of Water Supply: Research and Technology*, Vol. 49, No. 1, pp. 1-8.